

Solving PDE's with FEniCS

Stokes equation

Chapters 13–14

Introduction to
Automated Modeling
with FEniCS

by L. Ridgway Scott

The model equations for all fluids take the form

$$\mathbf{u}_t + \mathbf{u} \cdot \nabla \mathbf{u} + \nabla p = \nabla \cdot \mathbf{T} + \mathbf{f},$$

where \mathbf{u} is the velocity of the fluid, p is the pressure, \mathbf{T} is called the extra (or deviatoric) stress and \mathbf{f} is externally given data.

Models differ based on the way the stress \mathbf{T} depends on the velocity \mathbf{u} .

Time-independent models take the form

$$\mathbf{u} \cdot \nabla \mathbf{u} + \nabla p = \nabla \cdot \mathbf{T} + \mathbf{f}. \quad (1)$$

(Navier-)Stokes equations

For incompressible fluids, the equation (1) is accompanied by the condition

$$\nabla \cdot \mathbf{u} = 0, \quad (2)$$

which we will assume holds in the following discussion.

For suitable expressions for \mathbf{T} defined in terms of \mathbf{u} , the problem (1) and (2) can be shown to be well posed, as we indicate in special cases.

The simplest expression for the stress is linear:

$\mathbf{T} = \frac{1}{2}\eta(\nabla\mathbf{u} + \nabla\mathbf{u}^t)$, where η denotes the viscosity of the fluid.

Such fluids are called Newtonian.

(Navier-)Stokes equations

Scaling by η , (1) becomes

$$\frac{1}{\eta} \mathbf{u} \cdot \nabla \mathbf{u} + \nabla \hat{p} - \Delta \mathbf{u} = \hat{\mathbf{f}}, \quad (3)$$

where $\hat{p} = (1/\eta)p$ and $\hat{\mathbf{f}} = (1/\eta)\mathbf{f}$.

For η large, nonlinear term multiplied by η^{-1} often dropped, resulting in a linear system called the **Stokes equations** when (2) is added.

When the nonlinear equation is kept, equations (3) and (2) are called the **Navier-Stokes equations**, which we consider later.

Stokes equations

The Stokes equations for the flow of a viscous, incompressible, Newtonian fluid can be written

$$\begin{aligned} -\Delta \mathbf{u} + \nabla p &= \mathbf{0} \\ \nabla \cdot \mathbf{u} &= 0. \end{aligned} \tag{4}$$

in $\Omega \subset \mathbb{R}^d$, where \mathbf{u} denotes fluid velocity and p denotes pressure [5].

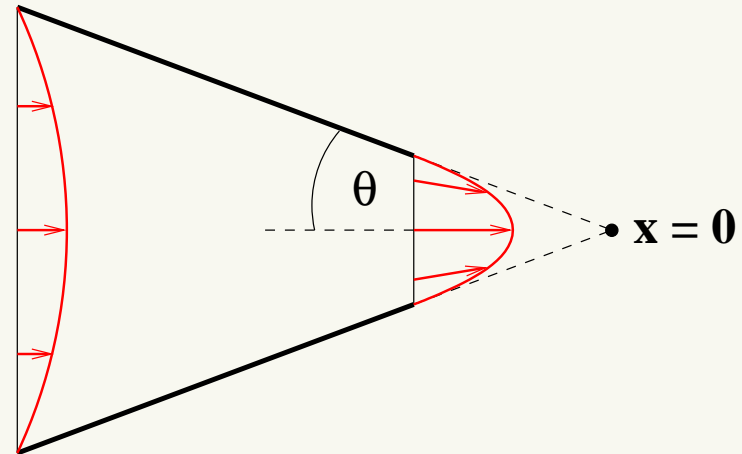
These equations must be supplemented by appropriate boundary conditions, such as the Dirichlet boundary conditions, $\mathbf{u} = \boldsymbol{\gamma}$ on $\partial\Omega$.

Continuity constraint, mass conservation

The key compatibility condition on the data comes from the divergence theorem:

$$\oint_{\partial\Omega} \boldsymbol{\gamma} \cdot \mathbf{n} \, ds = 0. \quad (5)$$

What goes in must come out:



Inhomogeneous boundary data can be dealt with by writing $\mathbf{u} = \hat{\mathbf{u}} + \boldsymbol{\gamma}$, where $\hat{\mathbf{u}}$ is in the usual variational space reflecting homogeneous Dirichlet data.

Stokes variational formulation

The variational formulation of (4) takes the form: Find \mathbf{u} such that $\mathbf{u} - \boldsymbol{\gamma} \in V$ and $p \in \Pi$ such that

$$\begin{aligned} a(\mathbf{u}, \mathbf{v}) + b(\mathbf{v}, p) &= 0 \quad \forall \mathbf{v} \in V, \\ b(\mathbf{u}, q) &= 0 \quad \forall q \in \Pi, \end{aligned} \tag{6}$$

where e.g. $a(\cdot, \cdot) = a_{\nabla}(\cdot, \cdot)$ and $b(\cdot, \cdot)$ are given by

$$a_{\nabla}(\mathbf{u}, \mathbf{v}) := \int_{\Omega} \sum_{i,j=1}^d u_{i,j} v_{i,j} d\mathbf{x}, \quad b(\mathbf{v}, q) := - \int_{\Omega} \sum_{i=1}^d v_{i,i} q d\mathbf{x}.$$

Derived by multiplying (4) by \mathbf{v} with a “dot” product, and integrating by parts as usual. Note that the second equation in (4) and (6) are related by multiplying the former by q and integrating, with no integration by parts.

Stokes variational spaces

The spaces V and Π are as follows.

In the case of simple Dirichlet data on the entire boundary, V consists of the d -fold Cartesian product of the subset of $H^1(\Omega)$ of functions vanishing on the boundary.

In this case, Π is the subset of $L^2(\Omega)$ of functions having mean zero.

The latter constraint corresponds to fixing an ambient pressure.

Another variational formulation for (4) can be derived which is equivalent in some ways, but not identical to (6).

Another Stokes variational formulation

Define

$$\epsilon(\mathbf{u})_{ij} = \frac{1}{2} (u_{i,j} + u_{j,i}) \quad (7)$$

and

$$a_\epsilon(\mathbf{u}, \mathbf{v}) := 2 \int_{\Omega} \sum_{i,j=1}^d \epsilon(\mathbf{u})_{ij} \epsilon(\mathbf{v})_{ij} \, d\mathbf{x}. \quad (8)$$

Then it can be shown that

$$a_\epsilon(\mathbf{u}, \mathbf{v}) := a_{\nabla}(\mathbf{u}, \mathbf{v}) \quad (9)$$

provided only that $\nabla \cdot \mathbf{u} = 0$ in Ω and $\mathbf{v} = 0$ on $\partial\Omega$
or $\nabla \cdot \mathbf{v} = 0$ in Ω and $\mathbf{u} = 0$ on $\partial\Omega$.

However, the natural boundary conditions associated with a_ϵ and a_{∇} are quite different [3].

Inhomogeneous boundary data dealt with by writing $\mathbf{u} = \hat{\mathbf{u}} + \boldsymbol{\gamma}$, $\hat{\mathbf{u}} \in V$, and (6) becomes

Find $\hat{\mathbf{u}}$ such that $\hat{\mathbf{u}} \in V$ and $p \in \Pi$ such that

$$\begin{aligned} a(\hat{\mathbf{u}}, \mathbf{v}) + b(\mathbf{v}, p) &= -a(\boldsymbol{\gamma}, \mathbf{v}) := F(\mathbf{v}) \quad \forall \mathbf{v} \in V, \\ b(\hat{\mathbf{u}}, q) &= -b(\boldsymbol{\gamma}, q) := G(q) \quad \forall q \in \Pi. \end{aligned} \quad (10)$$

From now on, we will drop the drop the “hats” on \mathbf{u} .

Mixed Method Formulation

The general formulation of the discretization (6) is of the form

$$\begin{aligned} a(u_h, v) + b(v, p_h) &= F(v) \quad \forall v \in V_h \\ b(u_h, q) &= G(q) \quad \forall q \in \Pi_h, \end{aligned} \tag{11}$$

where $F \in V'$ and $G \in \Pi'$ (the “primes” indicate dual spaces [2]).

It is called a “mixed method” since the variables v and q are mixed together.

For the Stokes problem (6), the natural variational formulation is already a mixed method, whereas it is an optional formulation in other settings.

Mixed Method Formulation

In the discrete mixed method, V and Π are two Hilbert spaces with subspaces $V_h \subset V$ and $\Pi_h \subset \Pi$, respectively.

The main twist in the variational formulation of mixed methods with inhomogeneous boundary conditions is that the term G is not zero [11].

We will assume there is a continuous operator $\mathcal{D} : V \rightarrow \Pi$ such that

$$b(v, p) = (\mathcal{D}v, p)_\Pi \quad \forall p. \quad (12)$$

In the Stokes problem, $\mathcal{D} = \nabla \cdot$.

Some details regarding inhomogeneous boundary conditions

Let P_Π denote the Riesz representation of G in Π_h , that is

$$(P_\Pi G, q)_\Pi = G(q) \quad \forall q \in \Pi_h. \quad (13)$$

Note that the second equation in (11) says that

$$P_\Pi \mathcal{D}u_h = P_\Pi G \quad (14)$$

where we also use $P_\Pi g$ to denote the Π -projection of $g \in \Pi$ onto Π_h .

Continuity and coercivity conditions

We assume that the bilinear forms satisfy the standard continuity conditions

$$\begin{aligned} a(u, v) &\leq C_a \|u\|_V \|v\|_V \quad \forall u, v \in V \\ b(v, p) &\leq C_b \|v\|_V \|p\|_\Pi \quad \forall v \in V, p \in \Pi. \end{aligned} \tag{15}$$

We also assume appropriate coercivity conditions

$$\begin{aligned} \alpha \|v\|_V^2 &\leq a(v, v) \quad \forall v \in Z \cup Z_h \\ \beta \|p\|_\Pi &\leq \sup_{v \in V_h} \frac{b(v, p)}{\|v\|_V} \quad \forall p \in \Pi_h. \end{aligned} \tag{16}$$

Note the special spaces Z and Z_h .

The spaces Z and Z_h

Z and Z_h are defined by

$$Z = \{v \in V : b(v, q) = 0 \quad \forall q \in \Pi\} \quad (17)$$

and

$$Z_h = \{v \in V_h : b(v, q) = 0 \quad \forall q \in \Pi_h\} \quad (18)$$

respectively.

Z is the set of divergence free functions in $H_0^1(\Omega)$, and

$$\mathbf{u} \in Z \text{ such that } a(\mathbf{u}, \mathbf{v}) = F(\mathbf{v}) \quad \forall \mathbf{v} \in Z.$$

Functions in Z_h are not in general divergence free, but

$$\mathbf{u}_h \in Z_h \text{ such that } a(\mathbf{u}_h, \mathbf{v}) = F(\mathbf{v}) \quad \forall \mathbf{v} \in Z_h.$$

Thus the variational problem for Stokes appears to be standard in the spaces Z and Z_h :

$$\mathbf{u}_h \in Z_h \text{ such that } a(\mathbf{u}_h, \mathbf{v}) = F(\mathbf{v}) \quad \forall \mathbf{v} \in Z_h.$$

But there is a variational crime in general: $Z_h \not\subset Z$.

So there are two things of concern:

- The approximate flow \mathbf{u}_h will not necessarily be incompressible, and
- we do not know if Z_h will provide good approximation.

Canonical variational form

The mixed formulation can be posed in the canonical variational form by writing

$$\mathcal{A}((u, p), (v, q)) := a(u, v) + b(v, p) + b(u, q) \quad (19)$$

$$\mathcal{F}((v, q)) := G(q) + F(v)$$

for all $(v, q) \in \mathcal{V} := V \times \Pi$.

This can be solved by direct methods (Gaussian elimination), **but the system is not positive definite.**

However, other algorithms can be used in special cases, as we discuss subsequently.

Taylor-Hood method

The first general spaces used for the Stokes equations (6) were the so-called Taylor-Hood spaces, as follows.

Let V_h^k denote C^0 piecewise polynomials of degree k on a triangulation T_h of a polygonal domain $\Omega \subset \mathbb{R}^d$.

Let

$$\tilde{V}_h = \left\{ \mathbf{v} \in (V_h^k)^d : \mathbf{v} = 0 \text{ on } \partial\Omega \right\} \quad (20)$$

and let

$$\Pi_h = \left\{ q \in V_h^{k-1} : \int_{\Omega} q(x) d\mathbf{x} = 0 \right\}. \quad (21)$$

It can be proved that (16) holds in both two and three dimensions under very mild restrictions on the mesh [1].

Note that $Z_h \not\subset Z$ in this case.

The main drawback of Taylor-Hood is that the divergence-free condition can be substantially violated, leading to a loss of mass conservation.

The loss of mass conservation can be avoided if we force the divergence constraint to be satisfied by a penalty method.

Taylor-Hood method limitations

Another drawback of Taylor-Hood is that the linear system (19) is bigger and not positive definite.

It represents a saddle-point problem.

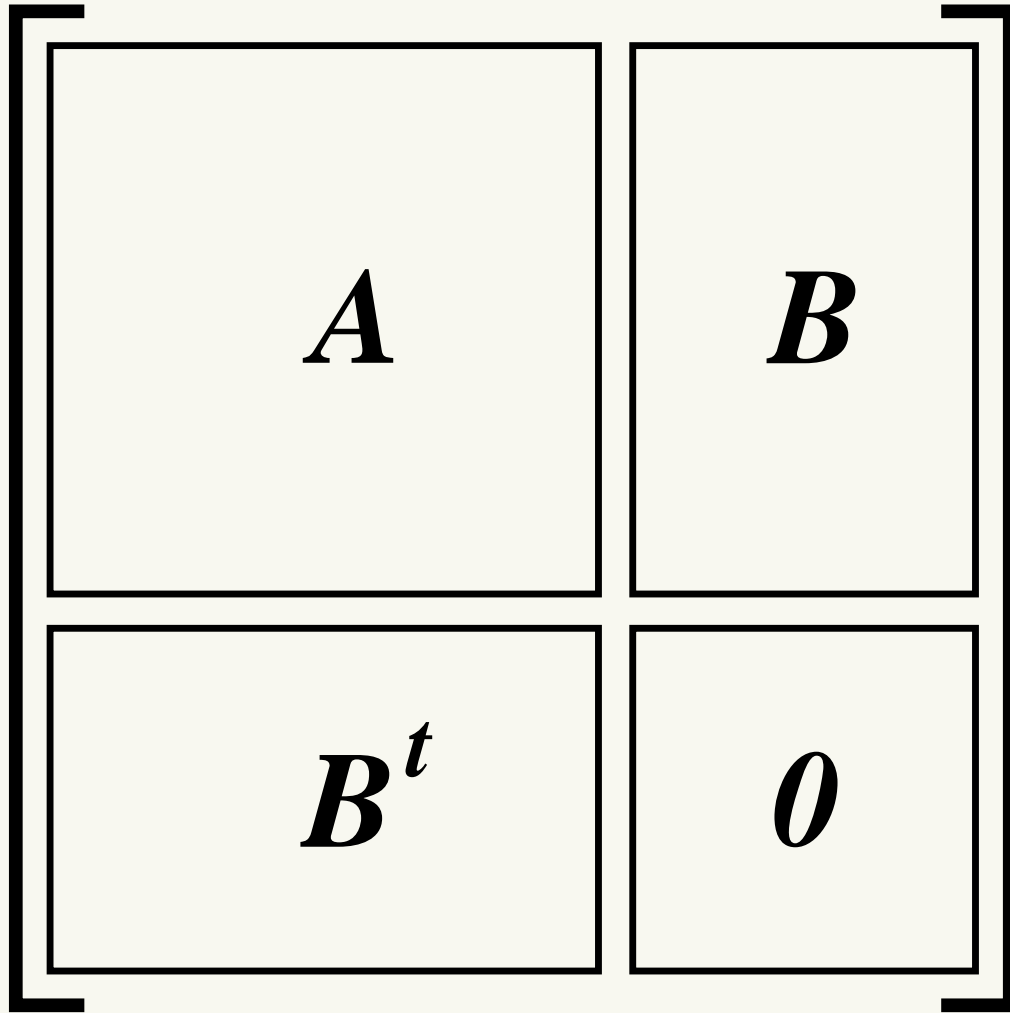
We will see that an iterated penalty method has a symmetric, positive definite linear system that is well conditioned.

Thus we consider the question of how to force $Z_h \subset Z$ for a general space V_h .

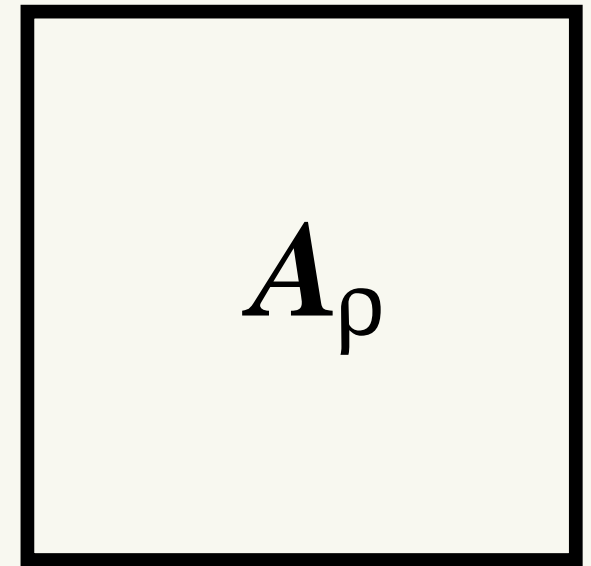
This can be done by choosing

$$\Pi_h = \nabla \cdot V_h.$$

Comparison of the matrix sizes



Taylor–Hood matrix



Iterated
Penalty
matrix

The discrete version of the Stokes equations can be written as

$$a(\mathbf{u}_h, \mathbf{v}) = F(\mathbf{v}) \quad \forall \mathbf{v} \in Z_h.$$

From Céa's theorem, the error $\mathbf{u} - \mathbf{u}_h$ is bounded by the best approximation from Z_h .

So the only issue is to see that the space Z_h is not over-constrained.

But in fact it can be.

Let us simply count the number of degrees of freedom for the mesh depicted in Figure 1.

Constraint counting

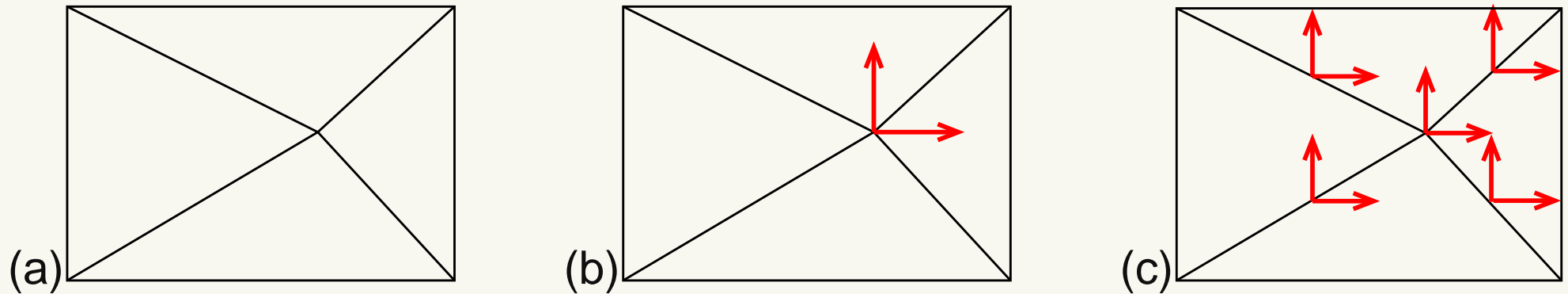


Figure 1: (a) A triangulation with only one interior vertex; (b) degrees of freedom for piecewise linear vector functions on this mesh that vanish on the boundary; (c) degrees of freedom for piecewise quadratic vector functions on this mesh that vanish on the boundary.

There are only two degrees of freedom, as indicated in Figure 1(b), for piecewise linear vector functions on this mesh that vanish on the boundary. That is, $\dim V_h = 2$.

If Π_h is piecewise constants on this mesh which have mean zero, then $\dim \Pi_h = 3$ (one for each triangle, minus 1 for the mean-zero constraint.)

Over constrained

Thus we see that the inf-sup condition (16) cannot hold; V_h is only two-dimensional, so the three-dimensional space Π_h must have p orthogonal to $\nabla \cdot \mathbf{v}$ for all $\mathbf{v} \in V_h$.

Moreover, it is not hard to see that $Z_h = \{0\}$, the space with only the zero function.

For V_h being piecewise quadratic vector functions on the mesh in Figure 1(a), the dimension of V_h is 10, as shown in Figure 1(c); there are 4 edge nodes and 1 vertex node, and 2 degrees of freedom for each.

If Π_h is discontinuous piecewise linears on this mesh which have mean zero, then $\dim \Pi_h = 11$ (three for each triangle, minus 1 for the mean-zero constraint.)

Reducing constraints

Thus we see that V_h is still too small to match Π_h , just by dimensional analysis.

One way to resolve this dilemma is to reduce the number of constraints implied by $b(\mathbf{v}, q) = 0$.

This could be done by making the pressure space smaller, or (equivalently as it turns out) reducing the accuracy of integration in computing $b(\mathbf{v}, q)$.

Such reduced or selective integration has been extensively studied [7].

But another way to eliminate the limiting behavior is to go to higher degree polynomials.

Higher-degree approximation

For V_h being piecewise quartic vector functions on the mesh in Figure 1(a), $\dim V_h = 50$ (there are 3 nodes per edge, 3 nodes per triangle and one vertex node).

Correspondingly, if Π_h consists of discontinuous piecewise cubics with mean zero, then $\dim \Pi_h = 39$ (10 degrees of freedom per triangle and one mean-zero constraint).

Thus we do have $\dim V_h \gg \dim \Pi_h$ in this case.

However, the counting of constraints has to be more careful.

Extract constraint counts

The divergence operator maps V_h to Π_h , with its image being W_h , and its kernel is Z_h . So

$$\dim V_h = \dim W_h + \dim Z_h.$$

We hope that $W_h = \Pi_h$, which is true if

$$\dim W_h = \dim \Pi_h = 39.$$

Thus we need to show that $\dim Z_h = 11$ in this case.

We can write $Z_h = \text{curl } S_h$ where

S_h is the space of C^1 (scalar) piecewise quintics

This space is specified uniquely by 11 parameters [9].

Convergence of Scott-Vogelius

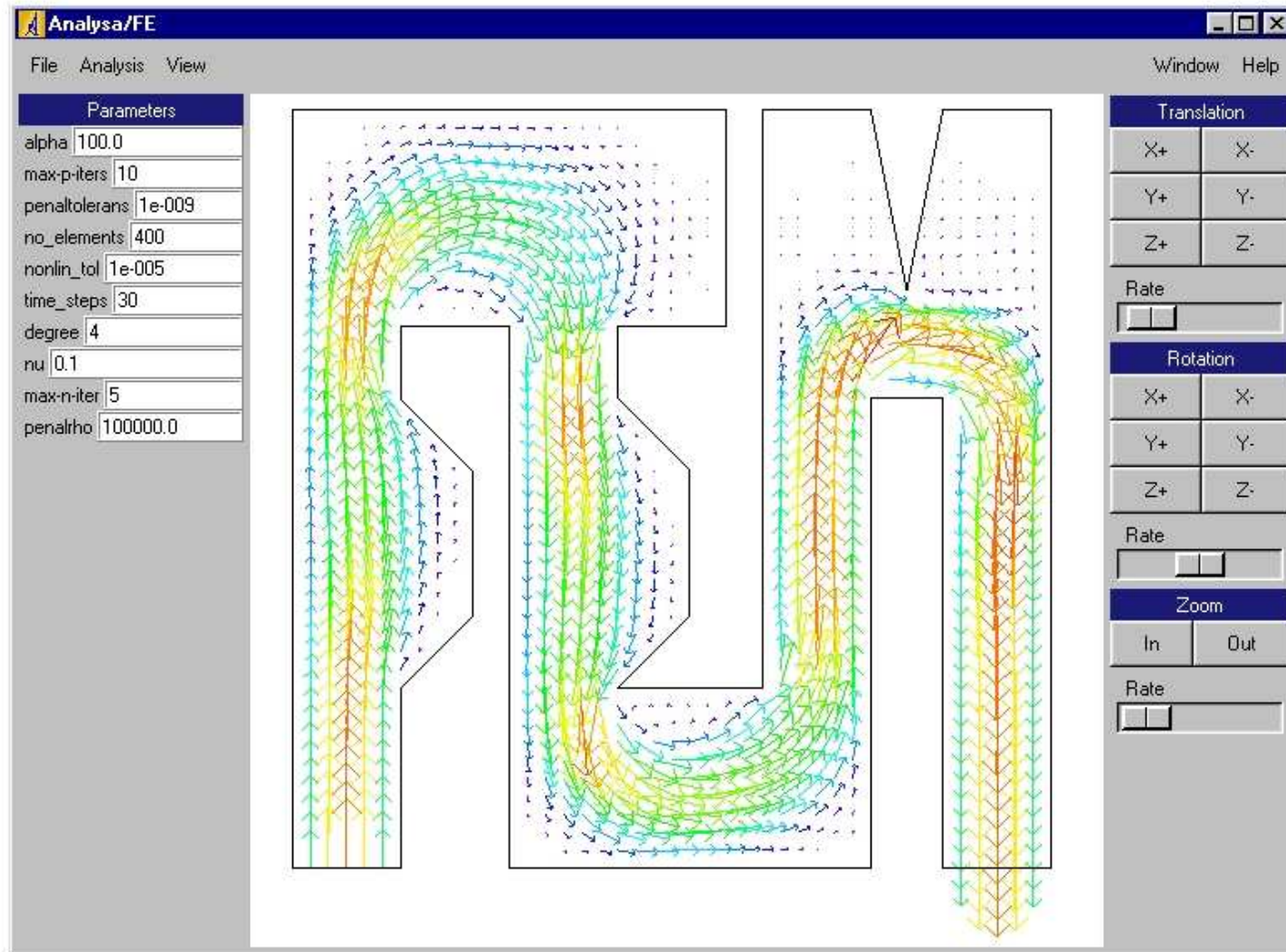
The choice of pressure space $\Pi_h = \nabla \cdot V_h$ is often called the Scott-Vogelius method.

The choice of pressure space $\Pi_h = \nabla \cdot V_h$ implies that $Z_h \subset Z$, and so the velocity error is governed by best approximation.

When the inf-sup condition holds with β independent of h , then best-approximation from Z_h may be related to best-approximation from V_h :

$$\begin{aligned} \|\mathbf{u} - \mathbf{u}_h\|_{H^1(\Omega)} &\leq \frac{1}{\alpha} \inf_{\mathbf{v} \in Z_h} \|\mathbf{u} - \mathbf{v}\|_{H^1(\Omega)} \\ &\leq \frac{C}{\alpha\beta} \inf_{\mathbf{v} \in V_h} \|\mathbf{u} - \mathbf{v}\|_{H^1(\Omega)}. \end{aligned} \tag{22}$$

Analysa using quartic elements and the iterated penalty method



Pressure convergence of Scott-Vogelius

When the inf-sup condition holds independently of the mesh, one also obtains the following approximation result for the pressure:

$$\|p - p_h\|_{L^2(\Omega)} \leq \frac{C}{\beta} \left(\inf_{\mathbf{v} \in V_h} \|\mathbf{u} - \mathbf{v}\|_{H^1(\Omega)} + \inf_{q \in \Pi_h} \|p - q\|_{L^2(\Omega)} \right).$$

Table 1 describes mesh restrictions under which the inf-sup bound (16) is known to hold with β independent of mesh size, in two and three dimensions, for various values of k .

Boundary singular vertices and nearly singular (interior) vertices are defined in [2, page 319].

The unified Stokes algorithm

Singular interior vertices (crossed triangles or crossed quadrilaterals) in the mesh are good (2D).

But inf-sup constant can degenerate if vertices are nonsingular close to being singular [2, page 319].

Scott-Vogelius algorithm produces a accurate velocity approximation with exact divergence zero, but pressure approximation is discontinuous.

By contrast, the Taylor-Hood pressure approximation is continuous but the velocity does not preserve mass.

The unified Stokes algorithm combines the best of these two methods and eliminates the bad features.

The unified Stokes algorithm defined

- The velocity approximation is exactly the same as for the Scott-Vogelius algorithm,
- but the pressure is obtained by projecting the Scott-Vogelius pressure onto the continuous pressure space (21) used in the Taylor-Hood method.

Scott-Vogelius pressure $p = \nabla \cdot \mathbf{w}$ for some $\mathbf{w} \in V_h$.

Then the unified Stokes pressure \hat{p}_h is defined by

$$(\hat{p}_h, q)_{L^2(\Omega)} = (\nabla \cdot \mathbf{w}, q)_{L^2(\Omega)} \quad \forall q \in \Pi_h.$$

Unified Stokes pressure \hat{p}_h defined by

$$(\hat{p}_h, q)_{L^2(\Omega)} = (\nabla \cdot \mathbf{w}, q)_{L^2(\Omega)} \quad \forall q \in \Pi_h.$$

We will show subsequently that \hat{p}_h is easy to compute, by identifying \mathbf{w} .

When the inf-sup condition holds independently of the mesh, the unified Stokes pressure \hat{p}_h also satisfies [8]

$$\begin{aligned} \|p - \hat{p}_h\|_{L^2(\Omega)} \leq \frac{C}{\beta} & \left(\inf_{\mathbf{v} \in V_h} \|\mathbf{u} - \mathbf{v}\|_{H^1(\Omega)} \right. \\ & \left. + \inf_{q \in \Pi_h} \|p - q\|_{L^2(\Omega)} \right). \end{aligned} \tag{23}$$

Mesh restrictions

Under mesh restrictions, convergence of velocity can be proved [13, 12, 10, 6]

d	k	inf-sup	mesh restrictions
2	1	NO, but	works for all crossed triangles
2	2	YES	some crossed triangles required
2	3	YES	new conditions [4] required
2	≥ 4	YES	no nearly singular vertices
3	≥ 6	YES	only one T_h known

Table 1: Mesh restrictions for exact divergence-free piecewise polynomials; d = dimension of Ω , k = degree of polynomials.

Taylor-Hood has no analog for the piecewise linear case

Malkus crossed triangles show that the inf-sup condition is not necessary for well-posed mixed method

Approximation by Z_h based on Powell C^1 piecewise quadratic element.

We now turn to an algorithm for solving for the velocity and pressure without dealing explicitly with the pressure space Π_h .

The algorithm is a general optimization technique called the iterated penalty method.

Iterated Penalty Method

Consider a mixed method for Stokes of the form (11):

$$\begin{aligned}a(\mathbf{u}_h, \mathbf{v}) + b(\mathbf{v}, p_h) &= F(\mathbf{v}) \quad \forall \mathbf{v} \in V_h \\ b(\mathbf{u}_h, q) &= G(q) \quad \forall q \in \Pi_h.\end{aligned}$$

Let $\rho' \in \mathbb{R}$ and $\rho > 0$. The iterated penalty method is

$$\begin{aligned}a(\mathbf{u}^n, \mathbf{v}) + \rho (\nabla \cdot \mathbf{u}^n, \nabla \cdot \mathbf{v})_{\Pi} &= \\ F(\mathbf{v}) - (\nabla \cdot \mathbf{v}, \nabla \cdot (\mathbf{w}^n + \rho \boldsymbol{\gamma}))_{\Pi} &\quad \forall \mathbf{v} \in V_h \quad (24) \\ \mathbf{w}^{n+1} &= \mathbf{w}^n + \rho' (\mathbf{u}^n + \boldsymbol{\gamma}),\end{aligned}$$

The pressure is defined by

$$p_h = P_{\Pi} \nabla \cdot \mathbf{w}_h, \quad (25)$$

where $\mathbf{w}_h := \mathbf{w}^n$ for terminal value of n .

Convergence properties

The convergence properties of (24) follow from [2].

Theorem 0.1 *Suppose that the forms (11) satisfy (15) and (16). for V_h and $\Pi_h = \mathcal{D}V_h$. Then the algorithm (24) converges for any $0 < \rho < 2\rho'$ for ρ' sufficiently large. For the choice $\rho = \rho'$, (24) converges geometrically with a rate given by*

$$C_a \left(\frac{1}{\beta} + \frac{C_a}{\alpha\beta} \right)^2 / \rho.$$

The following stopping criterion follows from [2].

Theorem 0.2 *Suppose that the forms (11) satisfy (15) and (16). for V_h and $\Pi_h = \mathcal{D}V_h$. Then the errors in algorithm (24) can be estimated by*

$$\|\mathbf{u}^n - \mathbf{u}_h\|_V \leq \left(\frac{1}{\beta} + \frac{C_a}{\alpha\beta} \right) \|\mathcal{D}\mathbf{u}^n - P_\Pi G\|_\Pi$$

and

$$\|p^n - p_h\|_\Pi \leq \left(\frac{C_a}{\beta} + \frac{C_a^2}{\alpha\beta} + \rho' C_b \right) \|\mathcal{D}\mathbf{u}^n - P_\Pi G\|_\Pi.$$

When $G(q) = -b(\gamma, q)$, then $P_\Pi G = -P_\Pi \mathcal{D}\gamma$ and since $\mathcal{D}\mathbf{u}^n \in \Pi_h$,

$$\begin{aligned} \|\mathcal{D}\mathbf{u}^n - P_\Pi G\|_\Pi &= \|P_\Pi \mathcal{D}(\mathbf{u}^n + \gamma)\|_\Pi \\ &\leq \|\mathcal{D}(\mathbf{u}^n + \gamma)\|_\Pi. \end{aligned} \tag{26}$$

Convergence and stopping criteria

The latter norm in (26) is easier to compute, avoiding the need to compute $P_{\Pi} G$.

We formalize this observation in the following result.

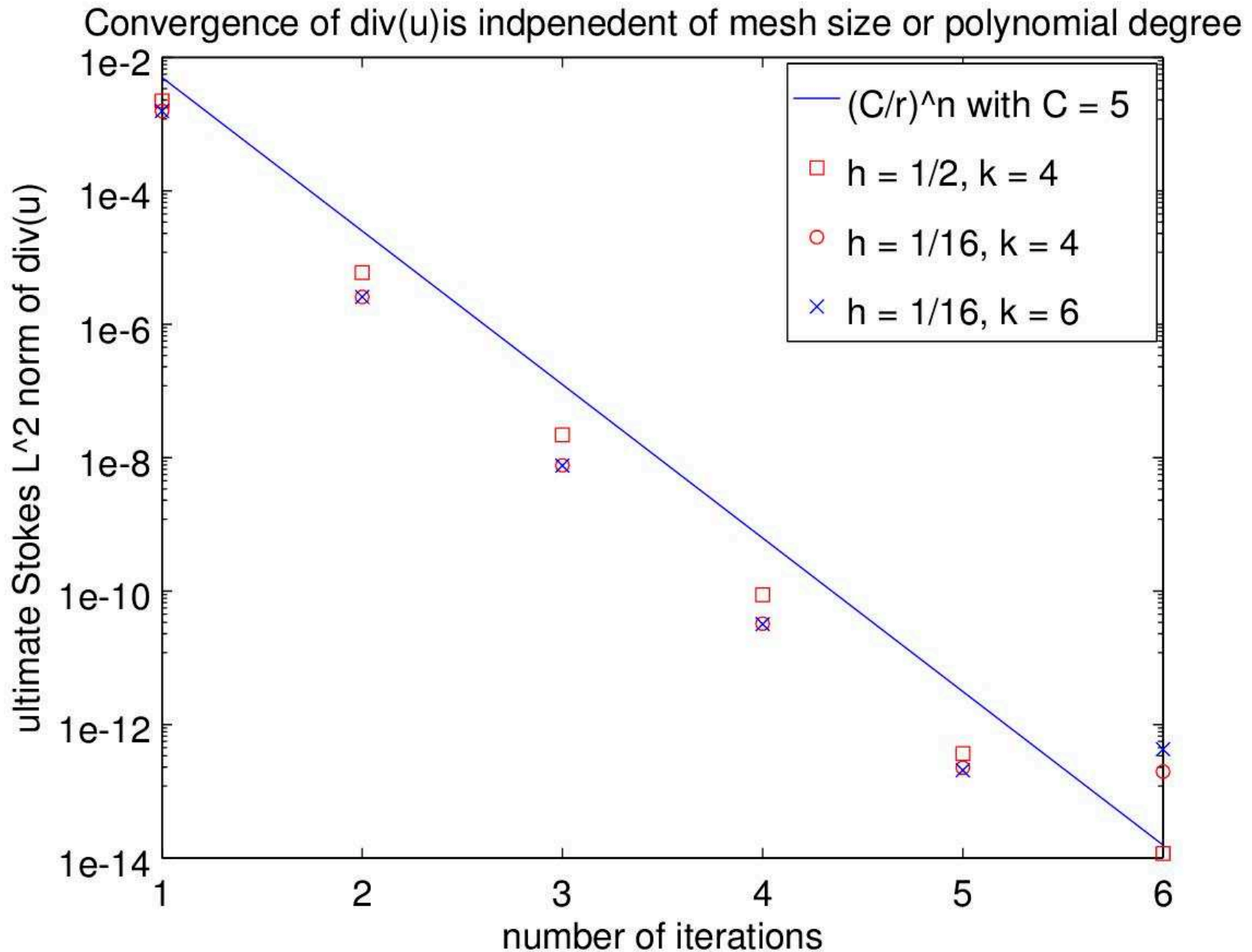
Corollary 0.1 *Under the conditions of Theorem (0.2) the errors in algorithm (24) can be estimated by*

$$\|\mathbf{u}^n - \mathbf{u}_h\|_V \leq \left(\frac{1}{\beta} + \frac{C_a}{\alpha\beta} \right) \|\mathcal{D}(\mathbf{u}^n + \boldsymbol{\gamma})\|_{\Pi}$$

and

$$\|p^n - p_h\|_{\Pi} \leq \left(\frac{C_a}{\beta} + \frac{C_a^2}{\alpha\beta} + \rho' C_b \right) \|\mathcal{D}(\mathbf{u}^n + \boldsymbol{\gamma})\|_{\Pi}.$$

Iterated penalty performance



The iterated penalty code

```
mesh = UnitSquareMesh(meshsize, meshsize, "crossed")
V = VectorFunctionSpace(mesh, "Lagrange", k)
u = TrialFunction(V)
v = TestFunction(V)
w = Function(V)
a = inner(grad(u), grad(v))*dx + r*div(u)*div(v)*dx
b = -div(w)*div(v)*dx
F = inner(f, v)*dx
u = Function(V)
pde = LinearVariationalProblem(a, F - b, u, bc)
solver = LinearVariationalSolver(pde)
# Scott-Vogelius iterated penalty method
iters = 0; max_iters = 10; div_u_norm = 1
while iters < max_iters and div_u_norm > 1e-10:
    # solve and update w
    solver.solve()
    w.vector().axpy(-r, u.vector())
    # find the L^2 norm of div(u) to check stopping condition
    div_u_norm = sqrt(assemble(div(u)*div(u)*dx(mesh)))
    print "norm(div u)=%.2e"%div_u_norm
    iters += 1
```

Test Problem

We can use FEniCS to test our algorithm. In our experiments, we try to recover an analytical solution of the Stokes equations

$$\mathbf{u} = \begin{bmatrix} \sin(4\pi x) \cos(4\pi y) \\ -\cos(4\pi x) \sin(4\pi y) \end{bmatrix}$$

$$p = \pi \cos(4\pi x) \cos(4\pi y)$$

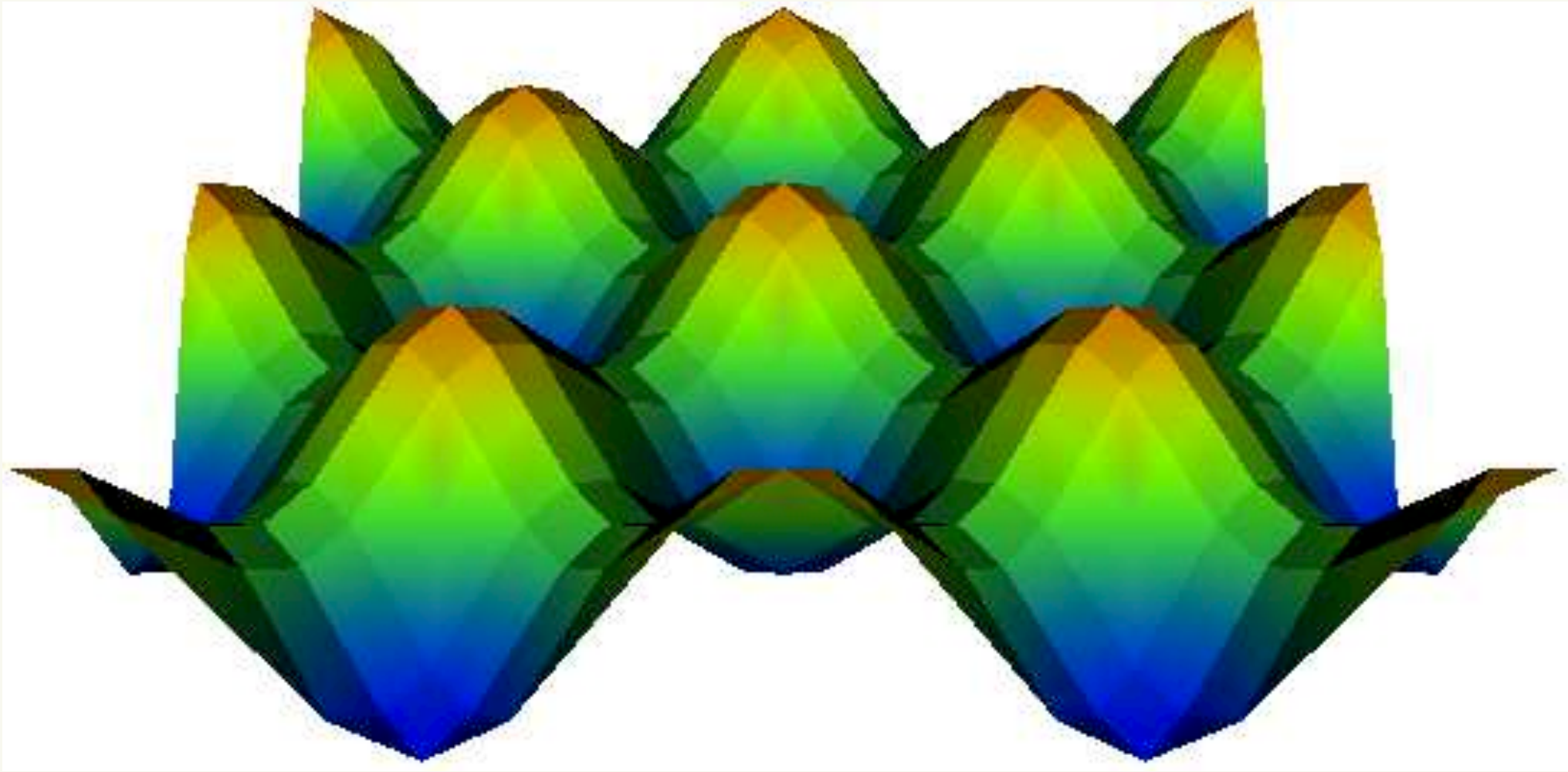
by applying \mathbf{u} above as a boundary condition and letting

$$\mathbf{f} = \begin{bmatrix} 28\pi^2 \sin(4\pi x) \cos(4\pi y) \\ -36\pi^2 \cos(4\pi x) \sin(4\pi y) \end{bmatrix}.$$

Next is a complete implementation on the unit square with mesh size $h = \frac{1}{16}$ and polynomial order $k = 6$.

Test Problem pressure

Unified Stokes solution for the pressure

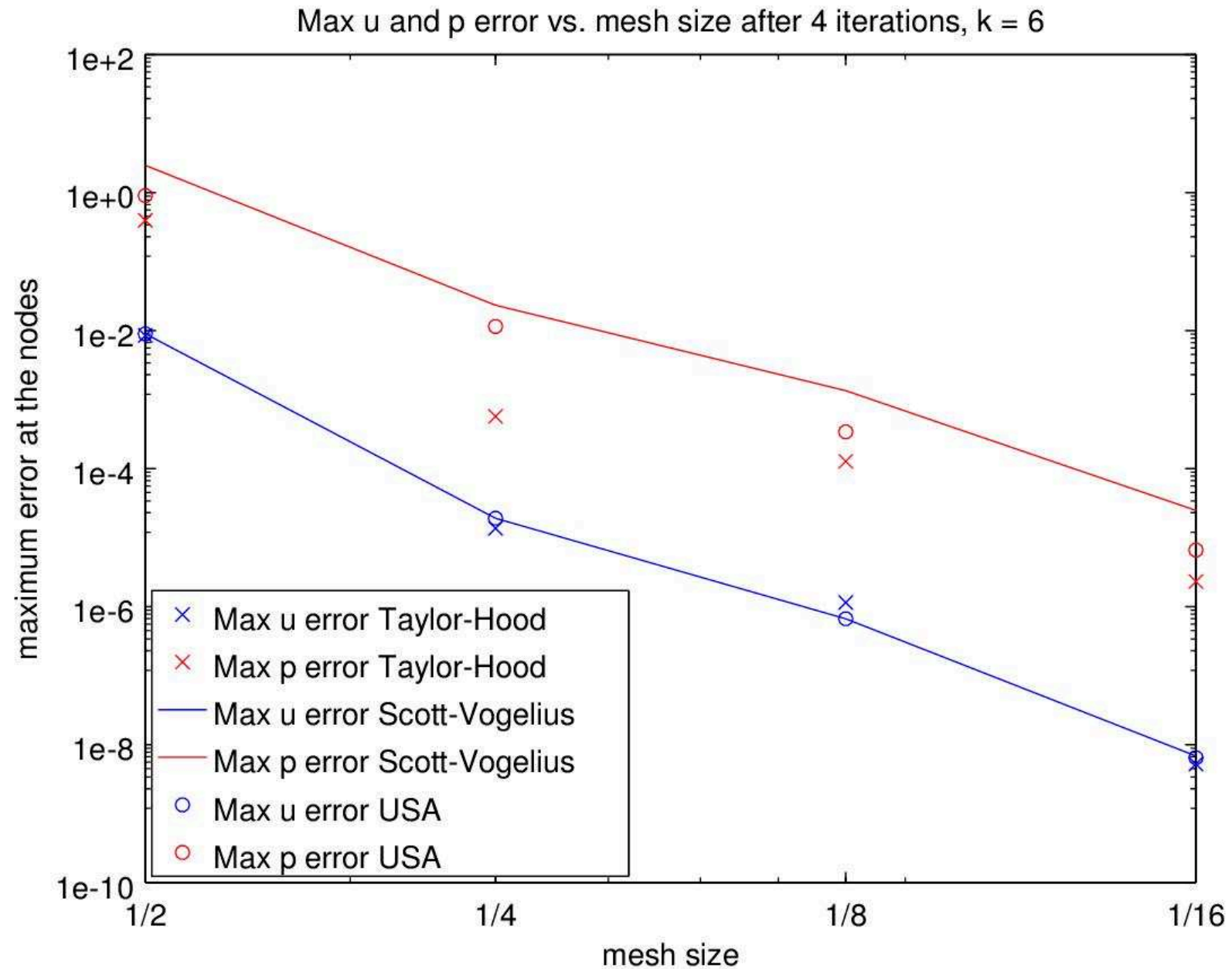


Divergence comparison

$\frac{1}{h}$	k	Taylor-Hood	Scott-Vogelius	Unified Stokes
2	4	1.86e-01	8.50e-11	4.27e-11
2	5	9.21e-02	7.24e-11	3.23e-11
2	6	3.60e-02	3.43e-11	3.33e-11
4	4	9.20e-03	3.46e-11	3.30e-11
4	5	3.52e-03	3.33e-11	3.28e-11
4	6	2.02e-04	3.24e-11	3.22e-11
8	4	6.41e-04	3.25e-11	3.20e-11
8	5	5.15e-05	3.17e-11	3.15e-11
8	6	4.67e-06	3.13e-11	3.12e-11
16	4	3.17e-05	3.14e-11	3.12e-11
16	5	9.99e-07	3.10e-11	3.09e-11
16	6	5.73e-08	3.09e-11	3.07e-11

Table 2: $\|\nabla \cdot \mathbf{u}\|_{L^2(\Omega)}$ for varying h and k with 4 iterations of the penalty method for Scott-Vogelius (and therefore also USA)

Numerical results



Stokes flow examples

We give here some important examples of Stokes flow.

- Poiseuille flow in a two-dimensional channel
- Poiseuille flow in a three-dimensional pipe
- Crossing channels
- Driven cavity

First two are elementary and exact

but also basis for many important applications.

We begin with flow in a channel.

Poiseuille flow

A two-dimensional channel Ω (a long rectangle) is an idealization of a canal.

We take the length to be L and the depth to be 1:

$$\Omega = \{ (x, y) \in \mathbb{R}^2 : 0 \leq x \leq L, 0 \leq y \leq 1 \}.$$

Restricting to two dimensions presumes that flow is negligible in third dimension across width of canal.

Flow in a channel is named for Poiseuille and defined by

$$\mathbf{u}(x, y) = \left(\frac{1}{2}y(1 - y), 0 \right), \quad \text{for } (x, y) \in \Omega. \quad (27)$$

$$\mathbf{u}(x, y) = \left(\frac{1}{2}y(1 - y), 0\right)$$

satisfies homogeneous Dirichlet boundary conditions on top and bottom of the channel:

we have put a lid on the canal.

If we write $\mathbf{u}(x, y) = (u(x, y), v(x, y))$, we see that v is identically zero, and u has a parabolic profile.

Moreover, $\Delta u \equiv 1$ and $\nabla \cdot \mathbf{u} = u_x = 0$. Thus define $p(x, y) = x$, and we have

$$-\Delta \mathbf{u}(x, y) + \nabla p(x, y) = 0 \quad \text{for } (x, y) \in \Omega.$$

Poiseuille flow in 3D too

Thus Poiseuille flow

$$\mathbf{u}(x, y) = (\tfrac{1}{2}y(1 - y), 0), \quad p(x, y) = x, \quad \text{for } (x, y) \in \Omega$$

satisfies the Stokes equations

$$-\Delta \mathbf{u}(x, y) + \nabla p(x, y) = 0 \quad \text{for } (x, y) \in \Omega,$$

$$\nabla \cdot \mathbf{u} = 0 \quad \text{for } (x, y) \in \Omega.$$

Three-dimensional flow in a pipe (cylinder) is similar and also is named for Poiseuille.

We can think of these flows as being driven by the non-zero pressure gradient.

Stokes cross

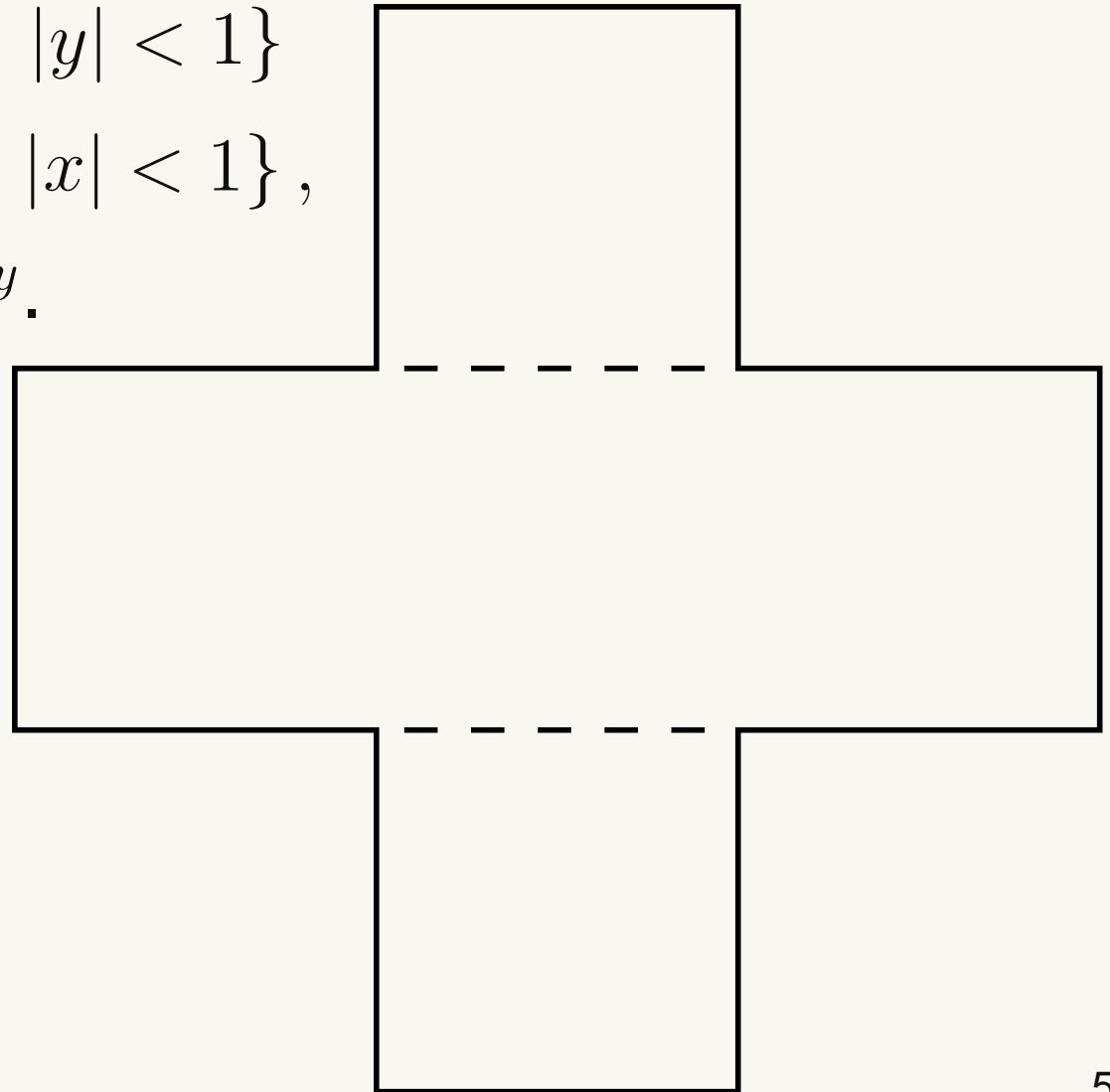
Now we consider two channels that cross each other.

Let $L \geq 1$. Define domains

$$\Omega^x = \{(x, y) : |x| < L, |y| < 1\}$$

$$\Omega^y = \{(x, y) : |y| < L, |x| < 1\},$$

and define $\Omega = \Omega^x \cup \Omega^y$.



Define vector functions

$$\mathbf{g}^x(x, y) = \begin{cases} (1 - y^2, 0) & |x| < L, \ |y| < 1 \\ \mathbf{0} & \text{elsewhere} \end{cases}$$

$$\mathbf{g}^y(x, y) = \begin{cases} (0, 1 - x^2) & |y| < L, \ |x| < 1 \\ \mathbf{0} & \text{elsewhere} \end{cases}.$$

By definition, $\mathbf{g}^x, \mathbf{g}^y \in H^1(\Omega)$, since

extension by zero is a continuous operation on H^1 .

Also $\nabla \cdot \mathbf{g}^x = \nabla \cdot \mathbf{g}^y = 0$ in Ω .

Similarly, define scalar functions

$$p^x(x, y) = \begin{cases} -2x & |x| < L, \ |y| < 1 \\ 0 & \text{elsewhere} \end{cases}$$

$$p^y(x, y) = \begin{cases} -2y & |y| < L, \ |x| < 1 \\ 0 & \text{elsewhere} \end{cases}.$$

These are both in $L^2(\Omega)$ and have mean zero.

In Ω^x , $-\Delta \mathbf{g}^x = (2, 0) = -\nabla p^x$, and

in Ω^y , $-\Delta \mathbf{g}^y = (0, 2) = -\nabla p^y$.

Stokes box

Then (\mathbf{g}^x, p^x) is a strong solution of Stokes in Ω^x ,
and (\mathbf{g}^y, p^y) is a strong solution of Stokes in Ω^y ,
with homogeneous Dirichlet boundary conditions on
appropriate sides of the two domains.

When $L = 1$ (Stokes box), $\Omega^x = \Omega^y$, and
both are solutions on all of Ω .

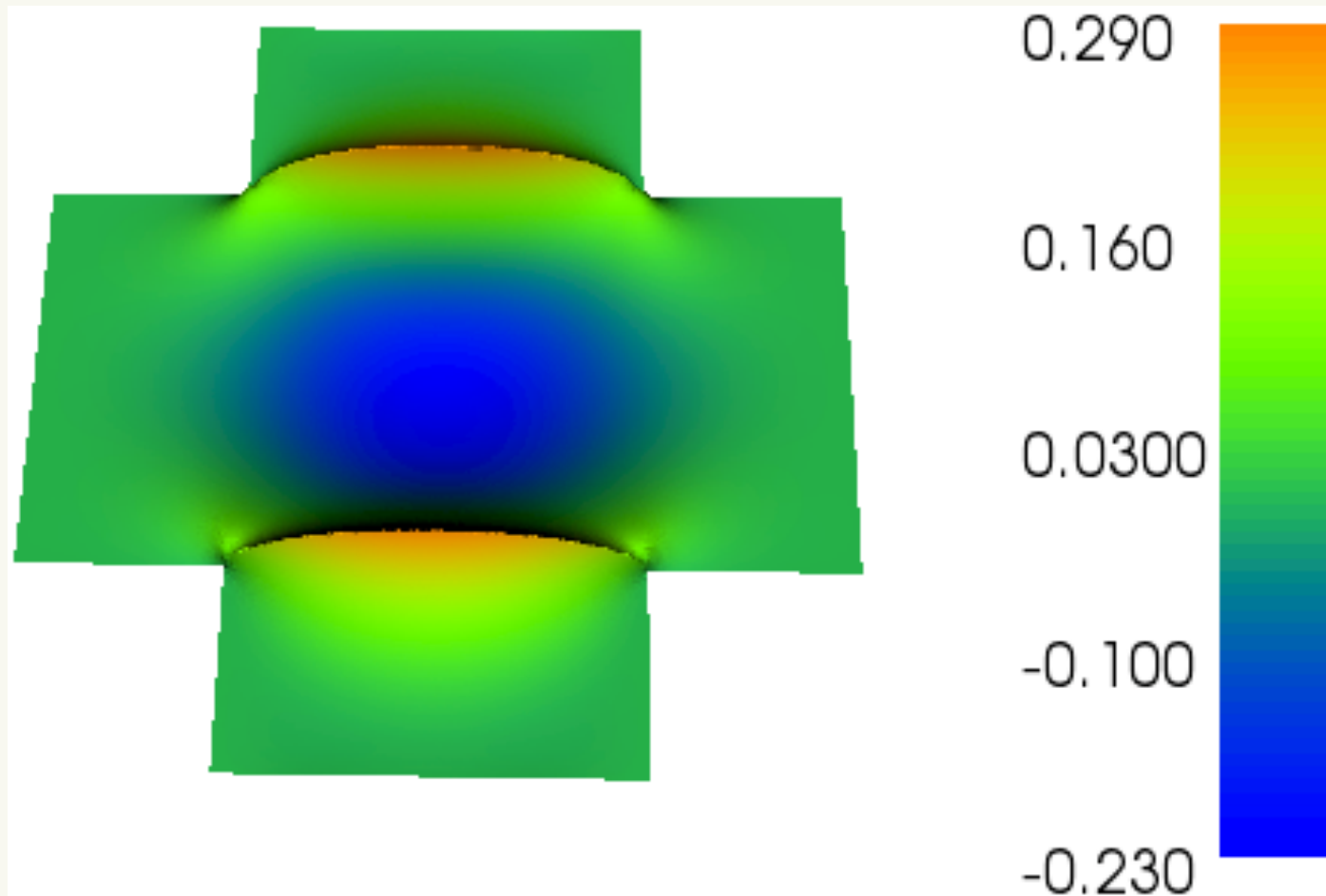
Thus any linear combination

$$(a\mathbf{g}^x + b\mathbf{g}^y, ap^x + bp^y)$$

is also an exact solution.

Stokes cross again

When $L > 1$, these do not give an exact solution.



Plot of $u_x - g_x^x$ where u has boundary data g^x .

(USA using $L=2$, quartics, and meshsize = 64).

Near solutions

How close are (\mathbf{g}^x, p^x) and (\mathbf{g}^y, p^y) to being solutions?

Extending p^x and p^y by zero outside of Ω^x and Ω^y , respectively, makes them both defined in $L^2(\Omega)$, still with mean zero in the whole domain.

Thus (\mathbf{g}^x, p^x) (resp., (\mathbf{g}^y, p^y)) is a strong solution of the Stokes equations in $\Omega \setminus B^x$ (resp., $\Omega \setminus B^y$), where

$$B^x = \{(x, \pm 1) : |x| < 1\} \quad \text{and} \quad B^y = \{(\pm 1, y) : |y| < 1\}$$

are the sets in Ω where both $\nabla \mathbf{g}^z$ and p^z ($z = x$ or y) have discontinuities.

Stokes cross

Let us determine what variational problem (\mathbf{g}^z, p^z) ($z = x$ or y) solves in Ω .

Take $z = x$ and let $\hat{\Omega}^y = \{(x, y) \in \Omega^y : |y| > 1\}$.

Thus $\Omega = \Omega^x \cup B^x \cup \hat{\Omega}^y$, and B^x is the boundary between Ω^x and $\hat{\Omega}^y$.

Since \mathbf{g}^x & p^x vanish in $\hat{\Omega}^y$, and \mathbf{v} vanishes on $\partial\Omega^x \setminus B^x$,

$$\begin{aligned} \int_{\Omega} \nabla \mathbf{g}^x : \nabla \mathbf{v} \, d\mathbf{x} - \int_{\Omega} p^x \nabla \cdot \mathbf{v} \, d\mathbf{x} &= \int_{\Omega^x} (-2y) v_{x,y} + 2x \nabla \cdot \mathbf{v} \, d\mathbf{x} \\ &= \int_{\Omega^x} (-2y) v_{x,y} \, d\mathbf{x} - \int_{\Omega^x} (2, 0) \cdot \mathbf{v} \, d\mathbf{x} - \oint_{B^x} (2x \mathbf{v}) \cdot \mathbf{n} \, ds. \end{aligned} \tag{28}$$

Applying the divergence theorem to $\mathbf{w} = (0, -2y)v_x$, we find

$$\int_{\Omega^x} (-2y)v_{x,y} d\mathbf{x} = \int_{\Omega^x} 2v_x d\mathbf{x} - \oint_{B^x} \mathbf{n} \cdot (0, 2y) v_x ds,$$

Thus

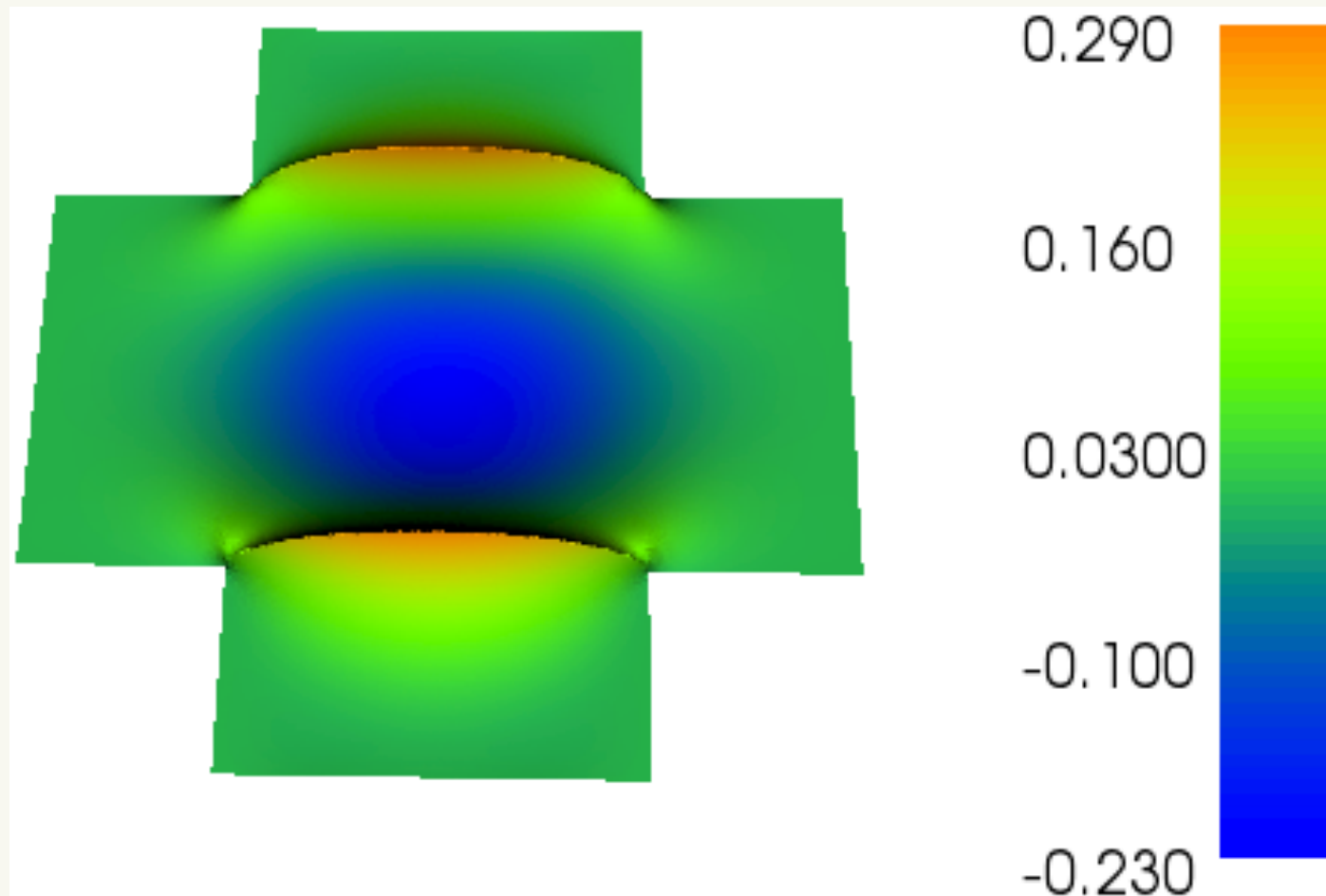
$$\begin{aligned} \int_{\Omega} \nabla \mathbf{g}^x : \nabla \mathbf{v} d\mathbf{x} - \int_{\Omega} p^x \nabla \cdot \mathbf{v} d\mathbf{x} = \\ - \oint_{B^x} \mathbf{n} \cdot (0, 2y) v_x ds - \oint_{B^x} (2x\mathbf{v}) \cdot \mathbf{n} ds, \end{aligned} \quad (29)$$

Define

$$F(\mathbf{v}) = - \oint_{B^x} \mathbf{n} \cdot (0, 2y) v_x + (2x\mathbf{v}) \cdot \mathbf{n} ds. \quad (30)$$

Stokes cross

(\mathbf{g}^x, p^x) solves Stokes on Ω with data F given in (30).



Difference between \mathbf{u} and \mathbf{g}^x is very localized near B^x .

Driven cavity

Let Ω be the unit square $[0, 1]^2$ and let Γ denote the top of the square:

$$\Gamma = \{(x, 1) : 0 \leq x \leq 1\}.$$

Define Dirichlet boundary conditions

$$\mathbf{u}(x, 1) = (1, 0) \text{ on } \Gamma, \quad \mathbf{u} = \mathbf{0} \text{ on } \partial\Omega \setminus \Gamma. \quad (31)$$

The resulting Stokes problem

$$-\Delta \mathbf{u}(x, y) + \nabla p(x, y) = 0 \quad \text{for } (x, y) \in \Omega,$$

$$\nabla \cdot \mathbf{u} = 0 \quad \text{for } (x, y) \in \Omega.$$

with boundary condition (31) is **driven cavity** problem.

Driven cavity

We imagine the top of the box to be a belt that is continuously moving to the right and causing the fluid to do the same.

Slightly unrealistic, but easy to state problem with unknown solution often used as a test [8].

It is equally difficult to write down a vector function $(g, 0)$ that satisfies (31).

In polar coordinates, write $g(r, \theta) = \cos \theta$ for r near 0.

Has right boundary conditions near left-hand side of lid, but not in $H^1(\Omega)$.

Driven cavity singularity

So the driven cavity problem has a singularity that correlates with the difficulty of forcing the belt down onto the top of the box.

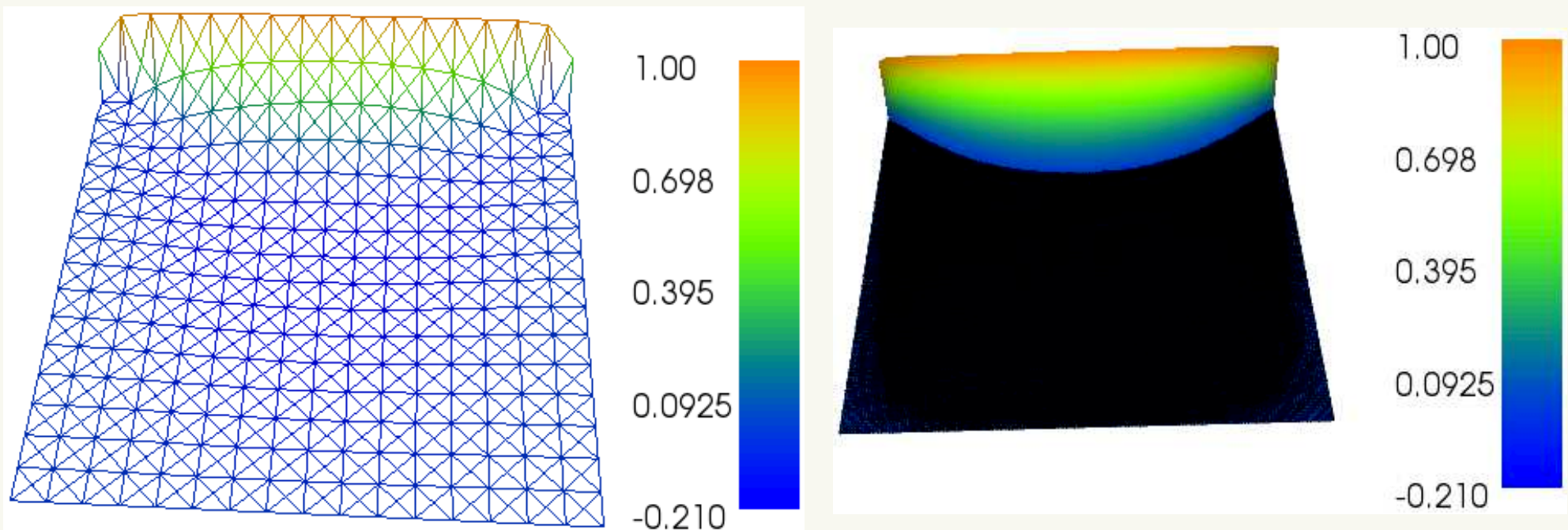


Figure 2: Driven cavity problem computed with quartics, horizontal component only. (left) meshsize = 16 and (right) meshsize = 128 showing only where $u \geq 0$. Computed with iterated penalty method using quartics.

Driven cavity

Horizontal component u of velocity $\mathbf{u} = (u, v)$ is plotted.

Horizontal velocity becomes negative below a particular curve.

This visualization was achieved by including the mesh, which is so dense as to appear black, and is plotted at the level $u = 0$.

Thus we see the solution only when it is positive.

The curve $u(x, y) = 0$ is a distinctive feature of this problem and can be used to compare solution methods.

References

- [1] D. Boffi. Three-dimensional finite element methods for the Stokes problem. *SIAM J. Num. Anal.*, 34:664 – 670, 1997.
- [2] Susanne C. Brenner and L. Ridgway Scott. *The Mathematical Theory of Finite Element Methods*. Springer–Verlag, third edition, 2008.
- [3] Max D. Gunzburger. *Finite Element Methods for Viscous Incompressible Flows*. Academic Press, 1989.
- [4] Johnny Guzmán and L. Ridgway Scott. Cubic Lagrange elements satisfying exact incompressibility. *SMAI JCM*, accepted, 2018.
- [5] L. D. Landau and E. M. Lifshitz. *Fluid Mechanics*. Oxford: Pergammon Press, second edition, 1987.
- [6] D. S. Malkus and E. T. Olsen. Linear crossed triangles for incompressible media. *North-Holland Mathematics Studies*, 94:235–248, 1984.
- [7] David S. Malkus and Thomas J. R. Hughes. Mixed finite element methods—reduced and selective integration techniques: a unification of concepts. *Computer Methods in Applied Mechanics and Engineering*, 15(1):63–81, 1978.
- [8] Hannah Morgan and L. Ridgway Scott. Towards a unified finite element method for the Stokes equations. *SIAM Journal on Scientific Computing*, 40(1):A130–A141, 2018.
- [9] J. Morgan and L. R. Scott. A nodal basis for C^1 piecewise polynomials of degree $n \geq 5$. *Math. Comp.*, 29:736–740, 1975.
- [10] Jinshui Qin. *On the convergence of some low order mixed finite elements for incompressible fluids*. PhD thesis, Penn State, 1994.
- [11] L. R. Scott, A. Ilin, R. Metcalfe, and B. Bagheri. Fast algorithms for solving high-order finite element equations for incompressible flow. In *Proceedings of the International Conference on Spectral and High Order Methods*, pages 221–232, Houston, TX, 1995. University of Houston.
- [12] L. R. Scott and M. Vogelius. Conforming finite element methods for incompressible and nearly incompressible continua. In *Large Scale Computations in Fluid Mechanics*, B. E. Engquist, et al., eds., volume 22 (Part 2), pages 221–244. Providence: AMS, 1985.